https://ntrs.nasa.gov/search.jsp?R=19690006586 2020-03-12T08:19:19+00:00Z

General Disclaimer

One or more of the Following Statements may affect this Document

- This document has been reproduced from the best copy furnished by the organizational source. It is being released in the interest of making available as much information as possible.

- This document may contain data, which exceeds the sheet parameters. It was furnished in this condition by the organizational source and is the best copy available.

- This document may contain tone-on-tone or color graphs, charts and/or pictures, which have been reproduced in black and white.

- This document is paginated as submitted by the original source.

- Portions of this document are not fully legible due to the historical nature of some of the material. However, it is the best reproduction available from the original submission.

Produced by the NASA Center for Aerospace Information (CASI)

THE APPLICATION OF THE SCANNING ELECTRON MICROSCOPE TO STUDIES OF CURRENT MULTIPLICATION, AVALANCHE BREAKDOWN AND THERMAL RUNAWAY

(I) - GENERAL PHYSICAL BASIS

by

P. R. Thornton, D. V. Sulway and D. A. Shaw

School of Engineering Science

U. C. N. W.,

Dean Street, Bangor,

Caerns., U. K.

University College of North Wales

NGR-52-117-001

N69-15918
(ACCESSION NUMBER)
43
(PAGES)
CR 99058
(NASA CR OR TMX OR AD NUMBER)
1
(THRU)
(CODE)
23
(CATEGORY)
FACILITY FORM 602

JAN 1969
RECEIVED
NASA STI FACILITY
INPUT BRANCH

The application of the scanning electron microscope to studies of current multiplication, avalanche breakdown and thermal runaway. (I) - General physical basis.

(I) Introduction

Scanning electron microscope studies of avalanche breakdown have already been reported in the literature (1),(2),(3),(4), and (5) . Usually these initial studies have been concerned with the qualitative detection and study of relatively gross but localised variations in current multiplication at voltages below the voltage, $\overline{V}_b$, at which the device breaks down. Under such conditions the device is thermally stable, the dark current flowing through the device is minimal and the difference in beam induced signal from the region of localised breakdown and the rest of the active area is large. Also there are no quantitative data in the literature and so the method is capable of considerable extension. In view of this and because of the potential of the method in the solution of practical problems it was considered worthwhile to establish the full worth of the method by examining both the quantitative extension and the extension to problems involving bulk breakdown and thermal runaway.

The main purpose of this paper is to establish the physical basis of the approach and to examine the practical limitations of the method.

The paper is divided into the following main sections:

(a) A qualitative discussion of the way in which current multiplication can lead to contrast in the scanning electron microscope (SEM).

(b) An assessment of the experimental systems that can be used to exploit these contrast mechanisms.

(c) A discussion of the problems involved in avalanche studies because of the variability in the noise behaviour.

(d) A short discussion comparing the application of the SEM to this and similar problems with the use of other techniques.

It should be emphasised that the treatment given here is intended to give a general background and not a detailed treatment of particular aspects. Although some topics are considered in detail other topics only have the problems outlined as the work is still in its early stages. Although the discussion throughout is limited to diode studies the method can be applied to breakdown processes in bulk devices such as Gunn diodes, for example and

to dielectric structures such as passivating layers and thin film capacitors.

(2) Contrast due to current multiplication

2(a) General

We are concerned here with the conductive mode of operation of the SEM in which current flow in a junction device due to the charge collection of the electron beam induced carriers by a depletion layer is used to study the device properties. The normal use of the conductive mode is illustrated in figures 1(a) and 1(b). A fraction of the electron-hole pairs created by the scanning electron beam are created in, or diffused to, the depletion layer where each pair is separated by the high electric field inherent in the depletion layer. The electrons flow towards the n-type contact and the holes flow towards the p-type layer. To a first approximation this process represents a charging-up of the 'condensor' represented by the depletion layer. This perturbation of the voltage across the junction is neutralised by current flow in the external circuit. This external current can be detected as a voltage change across a series load resistor and used to intensity modulate a CRT which is being scanned in synchronism with the primary electron beam. When the reverse

bias applied across the junction is high enough the beam induced carriers are accelerated to high energies so that they can cause 'impact ionization' i.e. the formation of further electron-hole pairs which in turn cause further ionization so that a multiplication of the beam induced current occurs in the manner depicted in figure 1(c). This is the effect with which we are concerned. To develop the method further we have to establish an equivalent circuit for the process. At the same time it is essential to establish the predicted voltage dependence of the charge collection process and to relate it to other processes occurring at the same time.

2(b) <u>The charge collection signal as a function of bias</u>

Figure 2(a) shows a first approximation equivalent circuit of the charge collection process. The depletion layer is represented by a capacitor, C_j, in parallel with a shunt resistance R_s which represents the leakage processes through the depletion layer. The junction is in series with the bulk resistance of the n- and p-type layers etc. This internal series resistance is denoted by R_L'. Finally, the external load resistance is denoted by R_L. We have neglected here any capacitance associated with the device contacts i.e. we are assuming the existence of ohmic contacts. In addition we have ignored the complexities introduced by stray capacities.

If the primary beam excitation followed by the charge collection process result in an instantaneous current $I_{(V)}$ flowing through the capacitor circuit at a diode bias, V a current I_{cc} given by

$$I_{(V)} = I_{(V)} \; R_s(V) / (R_s(V) + R_L(V) + R_L) \quad \ldots\ldots \text{eq. 1}$$

If the corresponding current from the same device element at zero applied bias is $I_{(0)}$ we can define the effective multiplication, M_{eff}, by

$$I_{(V)} = I_{(0)} \cdot M_{eff} = I_{(0)} \; M_{eff} \; R_s(0) / (R_s(0) + R_L'(0) + R_L)$$

$$\ldots \text{eq. 2}$$

Equations 1 and 2 enable us to predict the behaviour of I_{cc} as a function of applied bias. In particular it enables us to separate variations in I_{cc} due to changes in the charge collection process from those due to other processes. We should perhaps consider in more detail the exact meaning of R_s and R_L'. It should be remembered that we are dealing ultimately with a scanning system and are concerned with the way in which the current from a small given element of surface is detected. Therefore R_S and R_L' are, in fact, the local values of the shunt and series resistances and, in general, these parameters can vary across the active area and are not to be identified with diode shunt and series resistances.

The variation of I_{cc} with bias is shown schematically in figure 2(b). Region 1 may be termed the 'normal' voltage range where the bulk of the published work has been done. For small reverse biasses the resistances R_S and R_L' do not vary significantly with voltage and I_{cc} is either nearly constant or slowly increases as the bias is increased. The major contribution to this small increase arises from the increase in depletion layer width with applied bias. In region 2, where the device is forward biassed, the nett electric field falls and significant minority carrier injection occurs. The minority carrier injection opposes the charge collection process, so that the beam excitation is 'neutralised' by an internal process and the external signal falls. Or, in terms of equation 1 and figure 2(a), minority carrier injection decreases R_s compared to $(R_L' + R_L)$ so that the measured signal decreases. Usually at applied voltages approaching the 'built-in' voltage I_{cc} fades rapidly into the noise.

The remaining regions (3 to 6) are concerned with current multiplication. In region 3 the multiplication increases relatively slowly with bias. The total current flowing is small and R_s and R_L' are effectively independent of the applied voltage. (However, see section 2(c)). As a result there is an increase in I_{cc} with increase

in voltage which reflects the voltage dependence of the multiplication, M. This increase accelerates rapidly at voltages approaching the breakdown voltage of the devices because of the essentially exponential increase in M with increase in voltage. This rapid build-up in signal leads to very high signals (region 4) at the breakdown voltage, $\overline{V}_b$. Above the breakdown voltage the current flow through the device increases to such an extent that the shunt and series resistance vary and the multiplication decreases. (See section 3(c)). As a result the detected signal decreases with increase in bias(region 5.) Finally, the high diode current leads to Joule heating and to instabilities in the device and, because the current multiplication process is temperature dependent, to variations and 'drifts' in signal. (region 6)

The discussion above is concerned mainly with the signal from one area on the device i. e. the primary electron beam is considered to be stationary. If we now consider the case of a scanning electron beam we can establish the main factors which lead to contrast associated with multiplication. In terms of equation 1 the signal resulting from a scanning electron beam will vary from place to place because of local variations in the fraction of pairs collected at low biasses (variations in $I(o)_{cco}$), variations in the local value of the effective multiplication, M_{eff},

and changes in the effective values of R_S and R_L'. Finally, because $I(o)_{cco}$, M_{eff} and both R_s and R_L' are temperature dependent it is possible that local temperature changes arising from Joule heating can lead to contrast.

2(c) The effect of field emission

The possibilities of detecting field emission by scanning electron microscopy is a topic in its own right, but it is relevant to outline the possibilities here, as field emission is often intimately connected with avalanching in devices. In general field emission requires higher fields than avalanching and so tends to occur mainly in diodes with narrow depletion layers i.e. diodes with high doping levels in the bulk regions. In practical terms this means that diodes which breakdown below about 6 volts do so by tunnelling i.e. internal field emission, while those which breakdown in excess of 14 volts do so mainly by current multiplication. For diodes with breakdown voltages between these limits both mechanisms play a significant role (6). It is also possible that tunnelling has a wider role in that it may be operative in regions where the junction is not uniform. Consider for example the model illustrated in figure 1(d). Under certain conditions of applied voltage it is possible that the breakdown mechanism in the centre region is mainly by tunnelling and that the mechanism around the centre

is by avalanching. The size of the central tunnelling region can, in principle, vary with applied voltage and with temperature. Tunnelling can be taken account of in an initial manner in terms of the circuit of figure 2(a). The multiplication itself can decrease towards the centre as indicated in figure 1(e). In addition the tunnelling mechanism is, in fact, a source of carriers i.e. conductivity, and, as a result, can affect the local value of both the series resistance, R_L, and the shunt resistance, R_s.

These effects would produce contrast effects very similar to those arising from local temperature distributions (see section 3). There are two indications that can be used to separate these two possibilities. (a) A high degree of circular symmetry is probably indicative that temperature effects are important as built in variations are likely to be unsymmetrical; (b) a delay of seconds after application of a bias increment before the observed contrast is established may be indicative of a thermal delay. Whereas a rapid approach to the final state probably indicates that temperature effects are unimportant.

3. Experimental methods to study avalanche effects in the SEM

3(a) Introduction

In exploiting the SEM in this problem we need to establish methods to obtain both qualitative and quantitative data as quickly as possible.

Ideally we wish to

(1) take micrographs of the whole device and preselected areas of interest.

(2) Measure the charge collection signal as a function of bias from chosen points and selected areas.

(3) Make maps of the current multiplication as a function of bias.

(4) Extend (1), (2) and (3) to high currents by using pulsed conditions to avoid thermal effects.

(5) Incorporate safety circuits so that the conditions approaching thermal runaway can be studied.

Not all these methods have been exploited fully to date but it is of interest to discuss the various possibilities bearing particular attention to the ways in which quantitative data can be obtained reliably and quickly.

3(b) Intensity modulation of CRT

This is the standard method of obtaining micrographs. It is a very versatile system with variable gain, a facility for 'backing'off' the bulk of the signal so that the top of the signal can be examined at high gain and a non-linear element (and γ control) which attenuates the high signals compared to the low signals and so allows more detailed examination of the regions giving lower signals. It is this versatility

that makes it difficult to extend the method to make reliable quantitative measurements, as it is necessary to calibrate the gain, the degree of back-off and the departure from linearity. Three methods are currently in use to obtain two dimensional data. These are termed deflection modulation, the comparator technique (7) and what may be called contour plotting. Each of these finds application in avalanche studies. Consider deflection modulation (8) first. Strictly speaking this technique, which has been exploited previously in X-ray microanalysis and electron diffraction, does not exploit intensity modulation as the signal is fed to the Y plates together with the frame time base while the line time base is fed to the X plates. Figures 3(a) and (b) show the value and limitations of this approach. Figures 3(a) and (b) are displays taken of devices with a simple geometry. The display is pleasing in that it makes an immediate and clearly understandable impact. On the other hand if the technique is used with a device of more complex surface structure the display can have little or no use as it immediately rises interpretative problems. This is one limitation i. e. it is of value only for simple structures. A further limitation is that further processing is required to obtain quantitative information i. e. the values have to be measured off the film. As there are easier ways of obtaining the required data the method only has a limited application.

A more general method is to feed the video signal to the grid of a CRT through a comparator circuit which passes a constant value, if, and only if, the input signal lies within the range of a pre-chosen comparison signal. By varying the latter the comparison signal contours of constant signal can be obtained. Figure 3(c) shows such a set of contours and gives an immediate impression of the quality of the device. This approach does suffer from what might be termed an overquantisation of the data i.e. the information comes out in black and white signals only and it is necessary to obtain a normal micrograph to interpret some of the observations. However, it is reasonably versatile if somewhat laborious and is complementary to the contour tracing method which combines both quantitative information with the normal 'pictorial' information. The basis of the method is outlined in figure 4 and our experience with this method is based entirely on the recent work of Flemming (9). An input signal is fed to a threshold detecting circuit which feeds an output pulse to a logic circuit whenever the input signal falls outside either an upper or a lower limit. The number and sign of these pulses are counted, stored and used to generate a 'switch back' ramp in the manner shown in figure 4(b). This switch back ramp is fed in antiphase to the input circuit. As a result the signal is kept

within the preset limits (see figure 4(c)) and after further amplification is used to form a micrograph. On this micrograph the discontinuous jumps at B, C etc. give sharp changes in signal from 'high white' to 'black' and so represent a series of contours at known levels (e. g. 10mV or 10^{-9} amp levels). The 'greys' which occur between each jump contain the pictorial information which allows the quantitative data in the contours to be related to the surface detail. With an ability to vary the step height, a variable gain and, possibly a differential input a versatile system is available which can be calibrated with a variable sine or square wave. Figures 4(d) to (g) show actual results using this technique.

3(c) Measurements of multiplication

The discussion of the previous section was concerned solely with the relative behaviour of the whole device at a fixed bias, but, having located the areas of special interest, we need to examine the behaviour of these as a function of bias. A relatively straightforward way of doing this on a point to point bias is blocked out in figure 5. By using a stationary, chopped beam and 'ramping' the diode bias we can obtain charge collection plots of the form shown in figure 6(a). This approach has two limitations - one that it is a point by point method, and secondly, because the voltage ramp takes a finite time there is some uncertainty with regard to effects arising from temperature changes at the higher currents. The first of these difficulties is not a major limitation and, if needs be, can be

removed by using a step and repeat programme which automatically deflects the beam by a fixed amount and then repeats the diode bias voltage ramp. The presence of temperature effects can be determined by reversing the voltage ramp and seeing if any hysteresis has been introduced into the curve (as in figure 6(b)). (10). This hysteresis has its origin in the temperature dependence of the avalanche process. If hysteresis is found some method is isolating the effects due to local temperature rises has to be found.

Probably the best way of studying temperature effects is to use a pulse technique similar to that shown in figure 6(c). A modulated or a D. C. electron beam is used but the diode bias is pulsed with a low duty cycle. The voltage pulse developed across the load resistor is due to both the pulsed 'dark' current flowing in the device and the beam induced signal. The bulk of the dark current is backed off using a differential input amplifier. The leading edge of the diode pulse is used to start a delayed trigger or gate which passes only that part of the signal occurring between $f\tau_1$ and $(f + \Delta f)\tau_1$ where τ_1 is the pulse length and $f \ll 1$ and $\frac{\Delta f}{f} \ll \frac{1}{10}$. In this way we can build up a micrograph of the charge collection behaviour at a given interval $f\tau_1$ after the current has been applied. As the bias (pulse height) is increased the device can be protected by decreasing the duty cycle. .Within certain limitations of gain x bandwidth this facility is already available in the Tektronix 547 scope with, for example,

a type'D'differential plug-in unit. The approach does not enable us to investigate thermal effects right up to the onset of thermal runaway. At very highbiases the pulse length has to be reduced right down to submicrosecond duration. The normal amplifier systems have not got sufficient gain band width product and it is necessary to use the frequency conversion facility that is inherent in sampling units. Such units have sufficient back-off for this purpose so that the top of the signal can be studied. Instead of sweeping the sampling time through the cycle as is done in the strobing technique the sample is taken at a fixed time in the cycle, integrated for a fixed number of cycles and then displayed. In this way it is possible to extend the technique so that 100ns pulse lengths can be examined at 10ns intervals. This ability to study dynamic events is, of course, achieved at the expense of an increase in integration time.

Finally, we should not forget that we have cine-techniques available. This method can be used to photograph "one off" events occurring in time intervals of one second or longer.

5. Signal to noise ratio under avalanche conditions

5(a) General

If a primary beam delivers a current I_p of electrons of voltage V_p on a specimen giving a back scattering yield η and a secondary electron yield σ then a total wattage, W, is absorbed in the specimen

where W is given by

$$W = I_p V_p (1 - \eta V_p'/V_p - \gamma V_s/V_p) = F I_p V_p \qquad \text{eq 3}$$

In this equation V_p' is defined as the mean energy of the back scattered electrons and V_s is the mean energy of the secondary electrons. This excitation energy will create a distribution in depth, N(z), of electron hole pairs per second such that

$$N = \int N(z)dz = F I_p V_p / E_i \qquad \text{eq 4}$$

where E_i is the ionization energy in the target material. A fraction f of these pairs will be collected by the depletion layer of the junction device being studied and so contribute to the charge collection current. The magnitude of the current which flows as a result of this charge collection depends on the rate at which the charge is collected. The signal consists of three components in general - those carriers created in the depletion layer itself and those minority carriers created in the bulk regions and which subsequently diffuse to the junction. Figure 7 shows the time scales of the various events which occur during the excitation process. A primary electron will lose its energy by forming a plasma of electron hole pairs in about 10^{-10} seconds. Those electron hole pairs formed in the depletion will immediately begin to be separated and so contribute to the current flow. This contribution will be complete within a time τ_o where τ_o is given by

either (a) A weighted mean of the carrier lifetimes in the depletion layer, if the lifetimes are less than the transit time required by the carriers to cross the depletion layer

or (b) the transit time, if the lifetimes are longer than the transit time

or (c) if one carrier gets trapped, the value of τ_0 will be less than the transit time if the carrier remains trapped. If the carrier is subsequently released further current flow may occur

In silicon devices, which is our main preoccupation here, we are concerned with cases (a) and (b).

Those carriers created in the bulk and diffuse to the junction will reach the junction after delays which vary from practically zero up to several times the minority carrier lifetime. Subsequently they will be collected in times of the order of those given above.

One other time is important in this context and that is the time τ_a that the primary beam spends on one element of the device area. If the charge collection time is greater than τ_a there is a danger that both resolution and contrast may be adversely affected because, while the collection is occurring, the spot will have moved onto another element so that the tail of the signal from the first area will appear to come from the second leading to a loss in contrast and an

apparent merging of the elements

So far we have only considered the behaviour of the junction in isolation from the rest of the circuit. In particular we have assumed that the external circuit responses instantly to the unbalance caused by the charge collection process. This is equivalent to assuming that we can, in practice, measure the short circuit current generated by an isolated junction. In practice this is not the case. Returning to figure 2(a) we see that for significant signal to be detected in the amplifier circuit the major part of the beam induced excitation has to be neutralised in the external circuit rather than by internal processes through R_s. This implies certain limitations on R_s. If significant signal is to be obtained $R_s \gg R_L + R_L$ this is not always possible even with R_L very small. Under these conditions the observed signal can only be increased by increasing the primary current.

The above discussion shows how quickly the specimen response to the beam excitation, how trapping can effect the contrast and resolution unless some limit is imposed on the scanning speed. If trapping is absent the useful scanning speed is limited by the response time of the amplifier, by the noise problems introduced by low integration times i.e. by fast scans or by oscillations in the specimen (see section 5(e)). This is the background against which the signal to noise problem has to be considered.

5(b) Signal to noise ratio under non-avalanche conditions

If a beam of electrons of energy qV_p carries a current I_p and remains on a surface element for τ seconds, the number of electron hole pairs collected by the corresponding element of underlying junction is

$$N_t = \left(\frac{I_p}{q}\right)\left(\frac{qV}{E_1}\right) f(V_p)\, F(\eta,w)\tau \qquad \text{eq. 5}$$

where E_1 is the impact ionization energy of the specimen studied, $f(V_p)$ is the fraction of the created pairs that is collected by the junction and $F(\eta,w)$ takes account of the loss due to backscattering and second electron emission (see section 5(a)). Under these conditions the two main contributions to the noise are the shot noise on the signal itself (of magnitude $\sqrt{N_t}$) and the shot noise on the dark current, I_D, being passed by the diode. Of these two the latter is the bigger contribution. On this basis we can write the signal to noise ratio as

$$S/N = N_t (I_d \tau\, q)^{\frac{1}{2}} = \left(\frac{I_p}{q}\right)\left(\frac{q}{I_d}\right)^{\frac{1}{2}}\left(\frac{qV}{E_i}\right) f(V_p)\, F(\eta)\tau^{\frac{1}{2}} \ldots\ldots \qquad \text{eq. 6}$$

In general terms equation 6 implies that very good signal to noise ratio can be obtained with a primary beam of 10^{-11} amps injecting charge into a diode passing, say, 10^{-6} to 10^{-3} amps with frame times of between 1 and 100 seconds. This is observed in practice unless internal neutralisation processes cause $f(V_p)$ to fall, in effect, to a

very low value. The extension of this approach to avalanching conditions is not straightforward because of changes in the character of the noise.

5(c) Noise under avalanche conditions

The simplest way to understand the basic changes in the characteristics of the noise is to recall that in treatments of the shot noise problem the electrons contributing to the noise current are considered as independent particles flowing at random intervals. Under avalanche conditions a degree of correlation is introduced. As a result the current consists of a relatively few random 'bursts' of electrons instead of independent particles. As a result the noise increases at the onset of current multiplication because the root mean fluctuation in current increases. In brief each element of the device can, under avalanching conditions, be in one of two states, either it can be avalanching ("on") or not avalanching ("off"). If a carrier arrives at the element while the element is off then it stands at a finite chance of causing current multiplication of value M. If it arrives when the element is 'on' it causes no multiplication. Therefore the total noise current flow can be written as

$$I_n' = qN_n = \left\{ n\phi_1 M + n\,(1 - \phi_1) \right\} qr \quad \ldots\ldots\ldots \text{eq. 7}$$

when n is the number of carriers reaching the junction element per second and ϕ_1 is the fraction of time the element is 'off', ϕ_1 is a function of the applied bias. If we consider the case where $\phi_1 \rightarrow 1$ then since M>>1 the above expression reduces to $n\phi_1 Mq\tau$. To obtain an estimate of the increase in noise under avalanche conditions we can use the theory developed by Shockley and Pierce (11) to calculate the noise in electron multipliers. If we take an oversimplified view of the avalanche process and regard it as a two stage process - the arrival of n electrons onto the element followed by an overall multiplication M we can find a lower limit to the increase in noise due to avalanching. We know from Shockley and Pierce (11) that

$$\overline{(N_n - \overline{N}_n)^2} = \overline{M}^2 \overline{(n - \overline{n})^2}\tau^2 + \overline{n}\tau \overline{(M - \overline{M})^2} \qquad \text{eq. 8}$$

If the incident noise carriers follow a random distribution $\overline{(n - \overline{n})^2}\tau^2 = n\tau$ therefore

$$\overline{(N_n - \overline{N}_n)^2} = \overline{n}\,\overline{M}^2 \left[1 + \frac{\overline{(M - \overline{M})^2}}{\overline{M}^2}\right]\tau \geq \overline{n}\,\overline{M}^2\tau \qquad \text{eq. 9}$$

Since the current flow through the element is $I_n' = q\overline{N}_n = \overline{n}q\phi_1\overline{M}$ we obtain the expected fluctuation i.e. the noise as

$$(\overline{(N_n - \overline{N}_n)^2})^{\frac{1}{2}} = (\overline{n}\,\overline{M}^2\tau)^{\frac{1}{2}} \geq (I_n'\tau/q)^{\frac{1}{2}}\,\overline{M}^{\frac{1}{2}} \qquad \text{eq. 10}$$

Therefore, compared to the element passing the same current under non avalanching conditions, the noise is greater by $\overline{M}^{\frac{1}{2}}$ or more.

Therefore as the element nears its breakdown voltage (which can be defined as the voltage for which $Q_1 = \frac{1}{2}$) then the noise increases because both I_n^i and $\overline{M}$ increase. Once the breakdown voltage has been exceeded another situation develops.

Above the breakdown voltage the multiplication pulses begin to arrive so fast that they give the impression of a steady D. C. current with small 'dips' in it i. e. the element is continually 'on' except for short and rare intervals. As these small and rare intervals constitute the main fluctuation the noise drops. The development of this model for a uniform diode leads to a noise voltage given by $V^2_{RMS}(\text{noise}) \propto I^{-1}$ i. e. the noise voltage decreases as $I^{-\frac{1}{2}}$ beyond the breakdown voltage $\overline{V}_b$ (12). In practice the situation is more complex, in all but the smallest diodes, because the diodes consist of a distribution of elements with varying breakdown voltage (13). As a result the curve takes the form shown in figure 8. At $\overline{V}_b$ most of the elements avalanche and give the behaviour known in figure 8(a). At slightly higher voltages the 'tail' of the distribution start avalanching and give additional peaks (the case shown in figure 8(c)) or a departure from the $I^{-\frac{1}{2}}$ law (see figure 8(b)).

Finally, we should recall that microplasmas (regions of enhanced field) occur and have breakdown voltages below $\overline{V}_b$. As a result additional 'spikes' in the noise occur (see figure 8(d)).

5(d) Signal to noise ratio under avalanche conditions

The previous section indicates the types of noise behaviour observed under avalanche conditions. To calculate the signal to noise ratio we have to recall that the signal (i. e. electron beam induced) carriers have to compete with the noise carriers for a change to cause multiplication i. e. the probability that a beam induced carrier will cause significant multiplication depends on the relative numbers of beam induced and noise carriers reaching the element. If we neglect the carriers that arrive while the element is 'on' then we can write the beam induced and noise currents respectively as

$$I_s' = N_t (N_t/(N_t + N_N))\phi_1 M$$
$$I_n' = N_n (N_n/(N_t + N_t))\phi_1 M \qquad \text{eq. 11}$$

If we assume that the noise signal arises from the shot noise on both these components we have a signal to noise ratio S:N given by

$$S:N = N_t \phi_1 (N_t/(N_t + N_n))\tau \overline{M} \Big/ \left\{ \left(\frac{\tau}{q}\right) (I_s' + I_n') \overline{M} \right\}^{\frac{1}{2}} \qquad \text{eq. 12}$$

Finally, two other points should be mentioned. One concerns the behaviour with a modulated beam and the second concerns the temperature dependence of the noise. If a modulated beam is used

the coupling interaction outlined above means that the 'dark current' carriers become more effective in causing multiplication during the periods when the beam is off. As a result the noise current is modulated at the frequency of the primary beam and in antiphase with the beam. This noise signal will not be detected by a narrow band phase detector if we just use the in-phase component. Therefore, provided the factor $N_t/(N_t + N_n)$ is included in the signal term, the usual expression for the enhancement of signal to noise ratio by band width limitation is still valid.

The problem of temperature variation is complex. The noise behaviour is temperature dependent in certain cases. If the diode is small and obeys the idealised $I^{-\frac{1}{2}}$ law mentioned above the noise current is independent of temperature (13). However, if localised variations occur and cause significant departures from the $I^{-\frac{1}{2}}$ law there is a temperature dependence which varies with current in a quite complicated manner. Haitz (13) has recorded data indicating that the noise increases with increase in temperature at low currents and decreases at higher currents for a diode breaking down at 13V. On the other hand, Melchior and Strutt (14) have shown that the noise can decrease with increase in current at low currents for a diode breaking down at 18V.

5(e) Practical implications

The complexities outlined in the previous section have several implications in practice. They mean that

(1) There are regions of the current voltage curve (corresponding to the peaks) over which useful micrographs cannot be obtained. Often these are relatively limited in extent and by careful control of voltage it is possible to obtain micrographs just below and above the peak and so 'bracket' the 'forbidden zone'.

(2) Because of the large variation in noise any contribution to minimizing the noise is welcome. This requirement means that phase sensitive systems using tuned elements of relatively high Q find a role in this work.

(3) It is difficult to predict the behaviour of a given device. In addition to the noise problems outlined above the combination of device at, or near, breakdown and a scanning electron beam can lead to oscillatory effects which can take a variety of forms particularly if there is any tendancy towards an "S" type negative resistance in the current voltage curve. Figure 9 shows the type of behaviour observed under this condition. Figure 9(a) shows the structure used, while figure 9(b) illustrates the charge collection behaviour at the base-collector junction at voltages just below the 'knee' in the VI curve. The remaining micrographs are similar micrographs taken at the knee

to the curve. Figure 9(c) was taken with fast line scans. The information consists of a series of dots with associated tails. Figures 9(d) and (e) are similar micrographs taken with slow scan rates. A 'wave like' structure is introduced into the micrograph. Figures 9(f) to (h) were obtained at slightly reduced bias with intermediate line speeds and illustrate how the apparent location of the signal can be made to vary by changing the scan direction, the beam current, the transistor biassing. Similar variations can be obtained by changes in the external circuit elements included in the circuit. This can often be used to restore the display to its more form without the element of 'stochasticality' present here.

b. Comparison with other techniques

Although the application of the SEM to relatively deep quantitative studies of semiconductor materials and devices has only just begun it is of interest to compare its usefulness with other instruments used in studies of the avalanche process. We have the flying light spot technique, the infra-red microscope, the SEM, the microanalyser etc. to complement the conventional electrical measurements by providing localised information.

6(a) Comparison between the SEM and the travelling light spot

In terms of resolution, easy and variability of scanning, control and measurement of excitation level the SEM is preferable to the travelling light spot. In general terms the SEM gives a resolution in this application of 1,000Å to 3,000Å except at very high currents or low beam voltages. The excitation level can be varied by six orders of magnitude. To determine the excitation level one simple current measurement using a Faraday cage is needed. The resolution of a travelling light spot is fixed at the best, the control of scanning is limited or expensive if variability is required. It is difficult to vary and measure the excitation level over more than three orders of magnitude with a light beam and still retain the resolution unless a mask is used, in which case the range of penetration is limited. The ease with which an electron beam can be modulated at high speeds is probably greater than in the case of a light beam although the use of Kerr cells to modulate light beams has become more extensive in recent years and the use of microwave techniques to modulate high focussed electron beams has yet to be assessed.

The two situations in which the light beam has advantages are when it is required to inject carriers deep into the material (unlikely in the

present application) or when it is necessary to study the effect of ambient gases at relatively high pressure (i. e. approaching atmospheric) on the breakdown properties. With these problems the use of the SEM is limited to penetration depths of about 20/4 and to gas pressures of the order of a millimetre of Hg.

6(b) Comparison between the SEM and the infra-red microscope

The IR microscope measures relative temperatures with fair accuracy, with resolutions down to 7/4. The measurements are somewhat laborious. The method is sensitive to about 1°C but care is required if absolute measurements of temperature are required, particularly in regard to the use of the correct value for the surface emissivity. The SEM can only give information about temperature distributions indirectly, i. e. by studying the spatial and time variation some temperature dependent effect and, from the known temperature coefficient, estimate the temperature variation. So far the quantitative application of this technique has only just begun (15). In the present problem we can, in principle, use the temperature dependence of the avalanche process to investigate the temperature variation. Before we can fully exploit the resolution, the speed and ease of scanning of electron beams we have to use the infra red microscope to establish the worth of the SEM in this application and to calibrate the method. It is

most likely that, in the immediate future, the SEM and IRM will be used in a complementary manner in much the same way as the SEM and the X-ray microanalyser are exploited.

Acknowledgements

The authors would like to thank Dr. Peter Flemming for communicating his work on contour plotting prior to publication and to G. Whitman who helped to develop the system for this work.

References

1. I. G. Davies, K. A. Hughes, D. V. Sulway and P. R. Thornton, Solid State Electron., 9, 275, (1966).

2. J. W. Gaylord, J. Electrochem. Soc., 113, 753, (1966).

3. N. F. B. Neve, M. Sc. Thesis, U. C. N. W., Bangor, (1966).

4. P. R. Thornton, N. F. B. Neve, D. V. Sulway and R. C. Wayte Proc. I. E. E. E. 9th Annual Symposium on Electron, Ion and Laser Technology, Berkeley, California (Ed. R. F. W. Pease)

5. N. F. B. Neve, K. A. Hughes and P. R. Thornton, J. Appl. Phys., 37, 1704, (1967).

6. See, for example, H. Weinerth, Solid State Electron. 10, 1053, (1968).

7. See, for example, P. R. Thornton, 'Scanning electron microscopy' Chapman and Hall, (1968).

8. See, for example. P. N. Denbigh and C. W. B. Grigson, J. Sci. Inst., 42, 305, (1965).

9. P. Flemming. To be published, see also Abstracts of Conference on Scanning Electron Microscopy. Physics Society, Cambridge, July (1968).

10. D. V. Sulway and P. R. Thornton, Annual report on C. V. D. Contract No. 3622-66, U. C. N. W. Bangor (1967).

11. W. Shockley and J. R. Pierce, Proc. I. R. E., 26, 321, (1938).

12. M. E. Hines, I. E. E. E. Trans. Electron. Devices ED13, 158, (1966).

13. R. H. Haitz, J. Appl. Phys., 38, 2935, (1967).

14. H. Melchior and M. J. O. Strutt, Sci. Electrica, 9, 129, (1963).

15. D. V. Sulway and P. R. Thornton. To be published.

Captions to figures

Figure 1. (a) Schematic illustration of the use of electron beam induced carriers to give a charge collection current, (b) showing how, under non-avalanching conditions, each pair drifts under the effect of the local field, (c) showing a contrasting situation under avalanching conditions in which the initial pair are accelerated by the field and cause further pairs (indicated by small carriers), (d) and (e) showing how tunnelling can, in principle, complicate the interpretation of localised multiplication studies:- (d) idealised variation of junction thickness leading to both increase in local multiplication and field emission, (e) corresponding variation of multiplication.

Figure 2. (a) A first approximation equivalent circuit for the charge collection process, showing how the internal excitation current, I_{cco}, is related to the measured current, I_{cc}. (b) Schematic drawing show how the measured current (under constant excitation) can vary as a function of applied voltage

Figure 3. (a) and (b) deflection modulation displays of the charge collection signal under non-avalanche conditions from two planar diodes, (a) $V_{applied} = 0$ volts, (b) at 'knee' in VI curve. (c) Multi-exposure comparator display

of similar diode $V_{applied}$ = 9.91 volts, comparator set at 0.19 volts then increased by 0.1 steps up to 3.19 volts at centre.

(d) A conductive micrograph of a microplasma array taken under noisy conditions with normal intensity modulation display. (e) Same as (d) but taken with contour system. (N.B. The 'tearing' on this micrograph is due to the scan generator having limited performance at slow line scans)..

Figure 4. Illustrating the contour plotting system (9).
(a) typical continuous signal showing how it can be divided up into equal increments at B, C, D etc,
(b) quantised version of the signal shown in (a) obtained by counting the points B, C etc. and storing the signal;
(c) resultant signal obtained by compounding (d) with (b) in antiphase. (d) to (g) actual system in operation.
100 c.s signal, 3 volt steps output, clock frequency = 400 k c; (d) input signal = .2 volts, 4 steps, second trace shows counting pulses, (e) as (d) but with the second trace showing the quantised signal; (f) input signal = .85 volts, 16 steps; (g) limit of satisfactory behaviour, input signal = 2.4 volts, 48 steps.

Figure 5. Block diagram showing how the signal from a given location can be plotted as a function of bias.

Figure 6. (a) The behaviour of the measured charge collection signal as a function of bias, when thermal effects are unimportant; (b) As (a) but for the case where Joule heating introduces inertia into the curve; (c) block diagram showing how conductive micrographs can be obtained with a pulsed system in order to study the role of thermal effects.

Figure 7. Schematic diagram of the time scales of the various processes contributing to the charge collection process.

Figure 8. Illustrating how localised variations in breakdown voltage can lead to variations in noise behaviour. (a) The idealised distribution giving that $I^{-\frac{1}{2}}$ noise law; (b) the presence of a continuous 'tail' giving departures in the $I^{-\frac{1}{2}}$ law; (c) the presence of subsidiary peaks giving in the noise curve and (d) 'microplasmas' giving noise peaks at lower currents.

Figure 9. Complications due to beam induced oscillations in devices biassed at or near to breakdown. (a) the device studied, (b) charge collection micrograph of the collector base junction at V = 93 volts (the 'knee' in the VI curve and with fast line scans (arrow indicates the direction of the line scan); (d) and (e) are micrographs taken under similar conditions to (c) but with slow line scans; (f) to (h) similar micrographs to (d) and (e) taken at suitable line speeds but with different circuit conditions, (f) with emitter base short-circuited, (g) with emitter base forward biassed and (h) with raster scan directions rotated through 90^{o}.

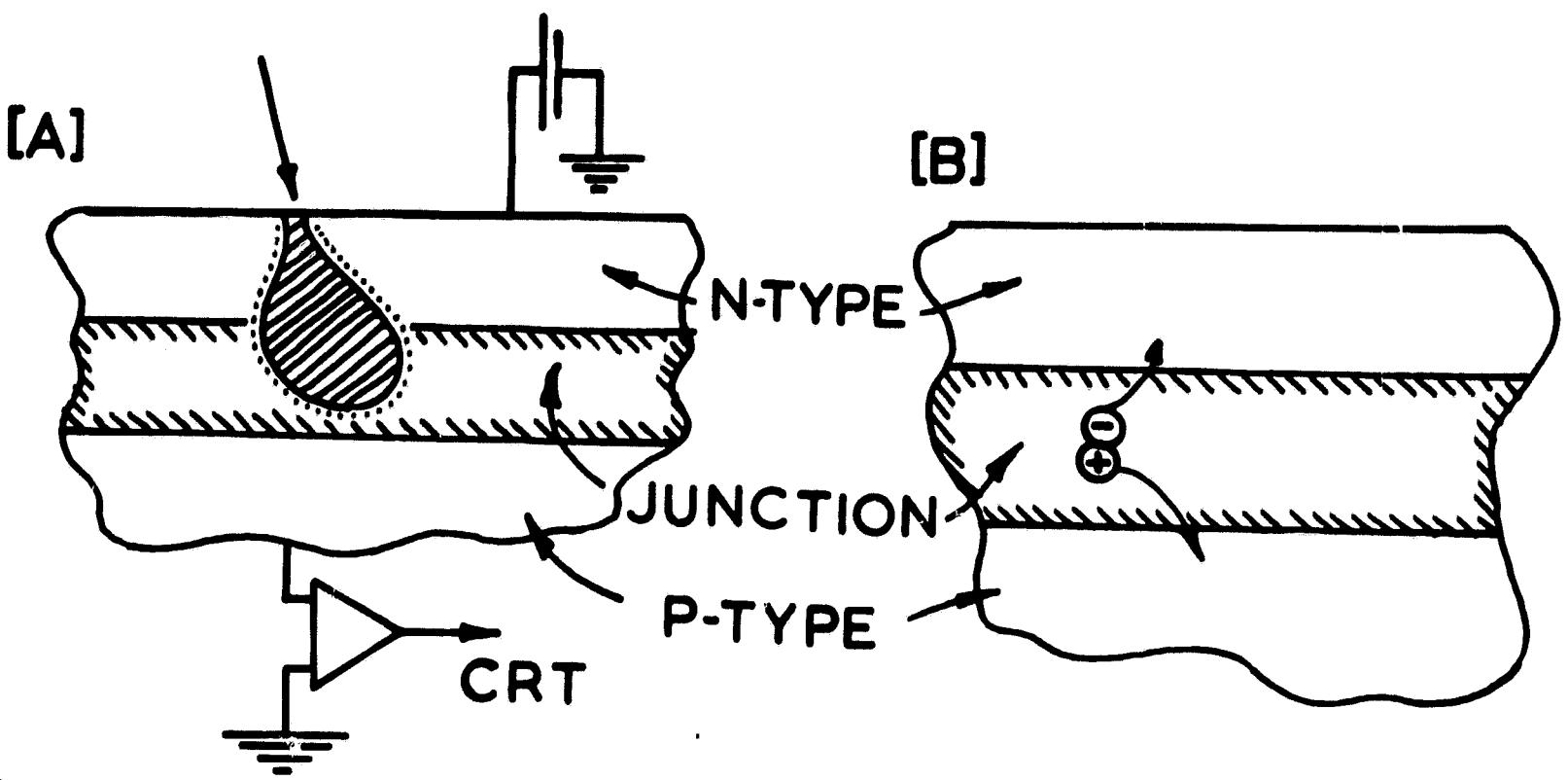
[A]
[B]
N-TYPE
JUNCTION
P-TYPE
CRT

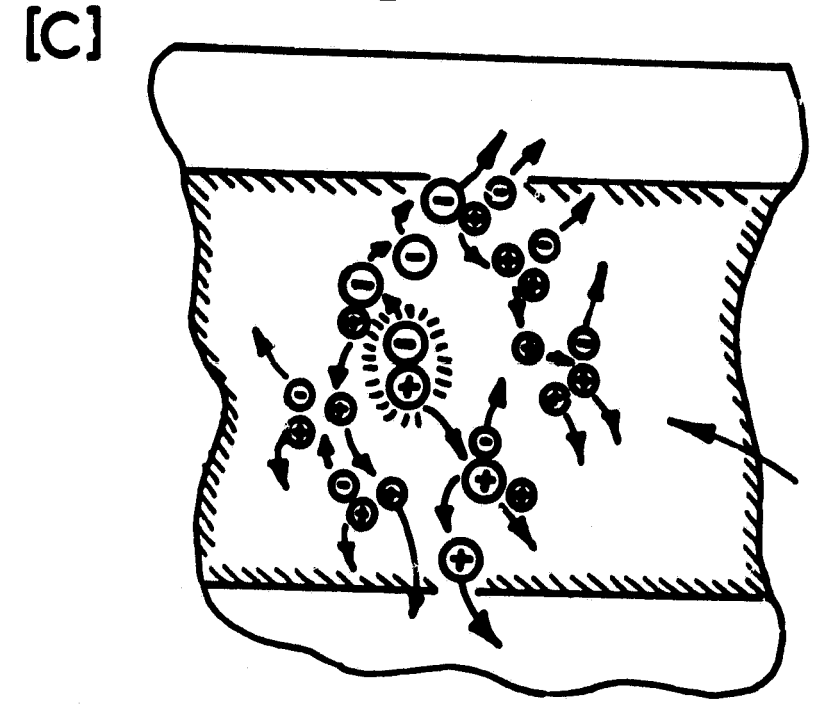
[C]
DEPLETION
LAYER

FIGURE.I.

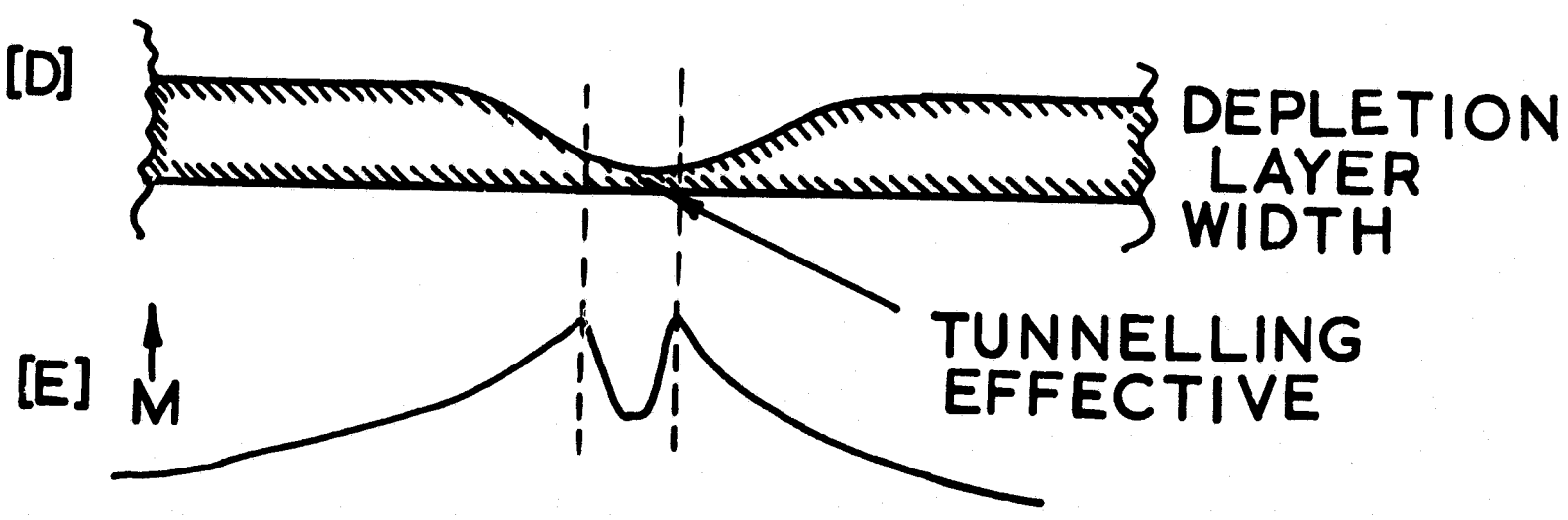
[D]
DEPLETION
LAYER
WIDTH
[E]
M
TUNNELLING
EFFECTIVE

FIGURE.2a.

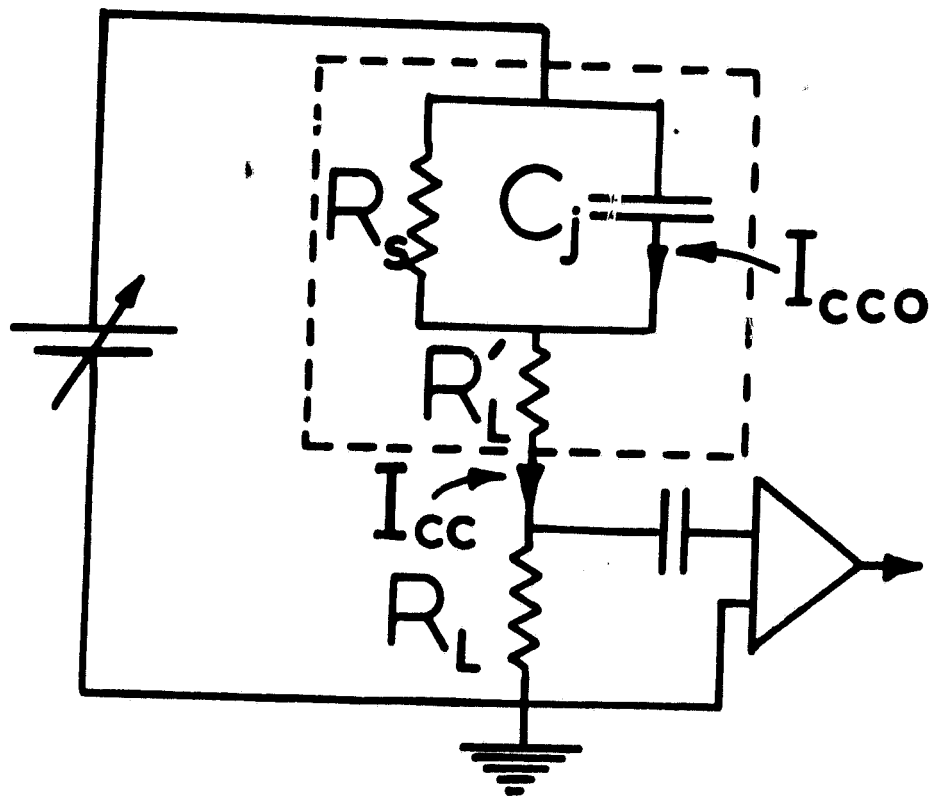

FIGURE.2b.

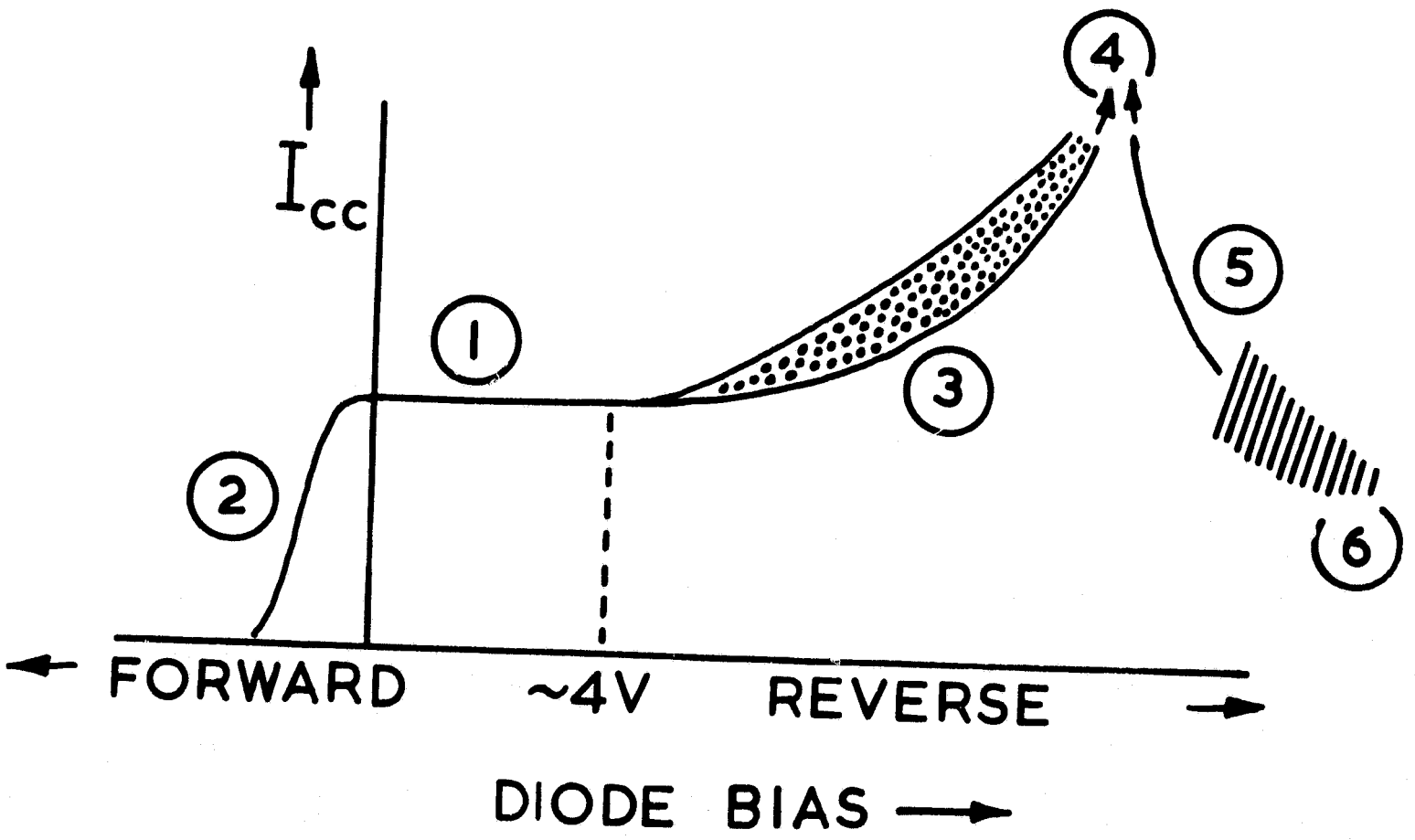

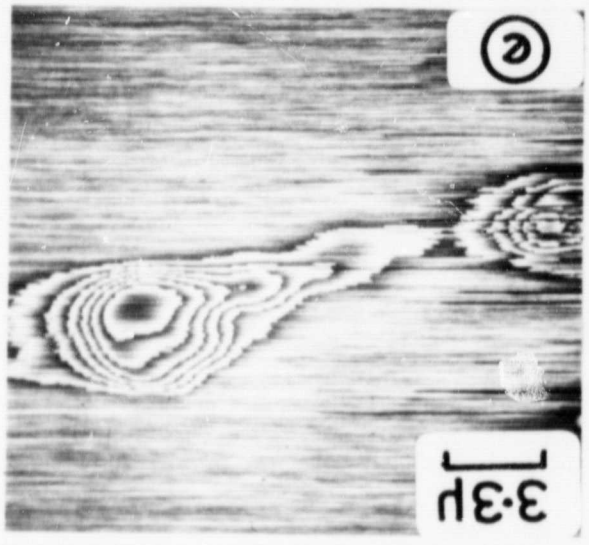

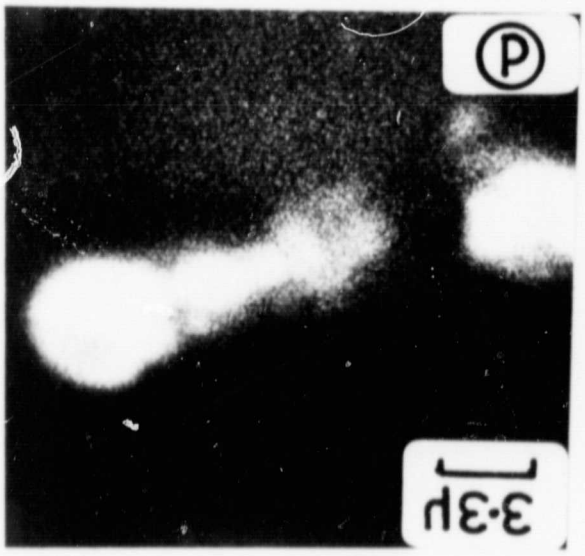

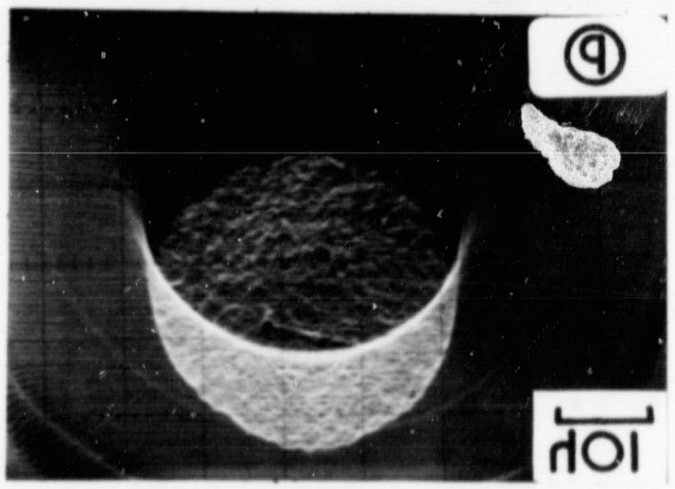

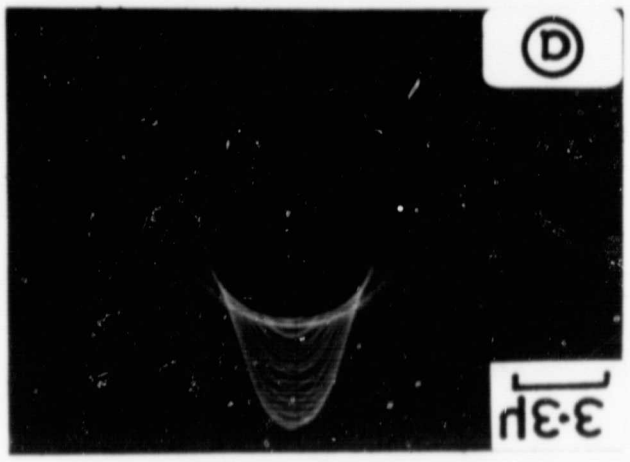

FIGURE.3.

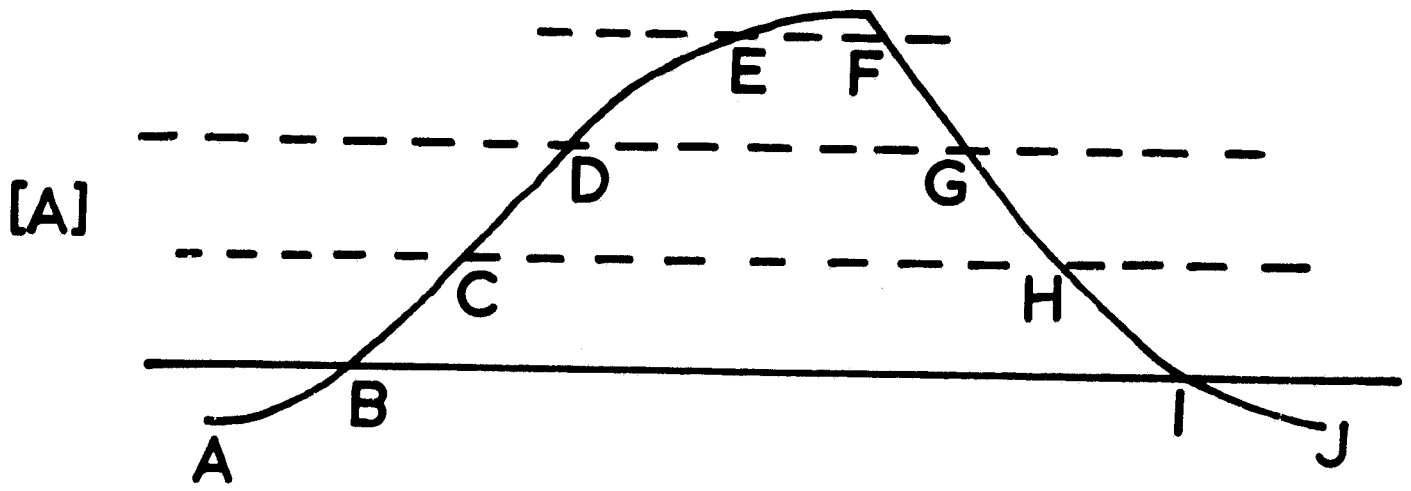

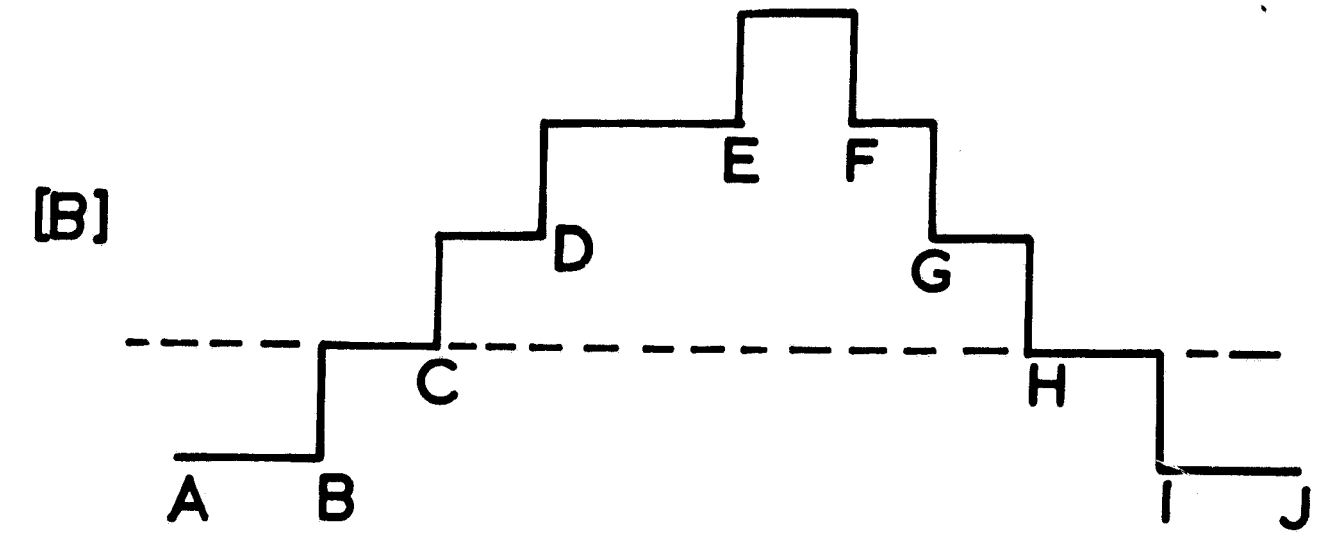

FIGURE.4.

FIGURE 4.
CONT:-

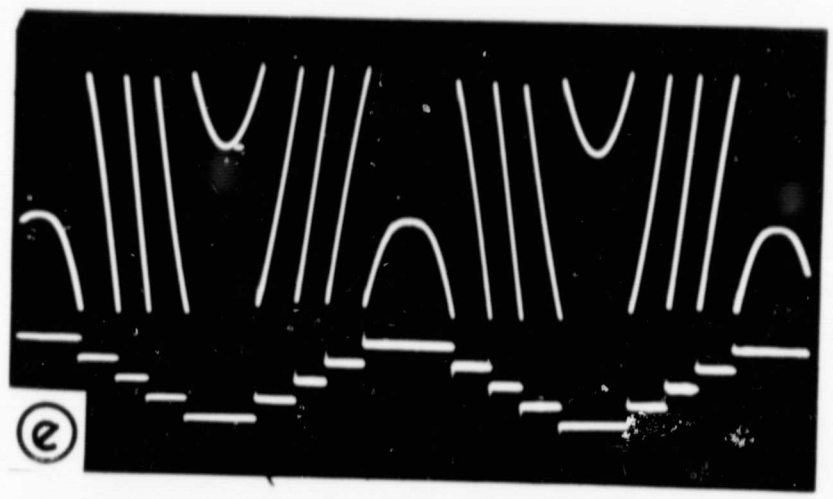

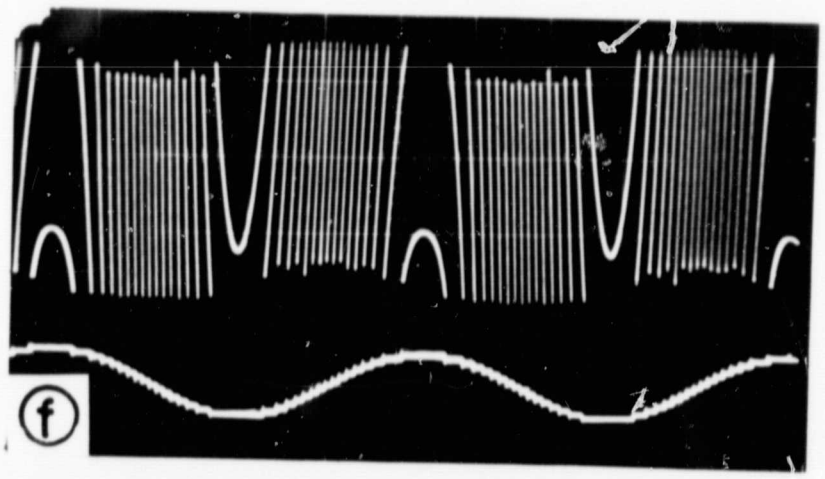

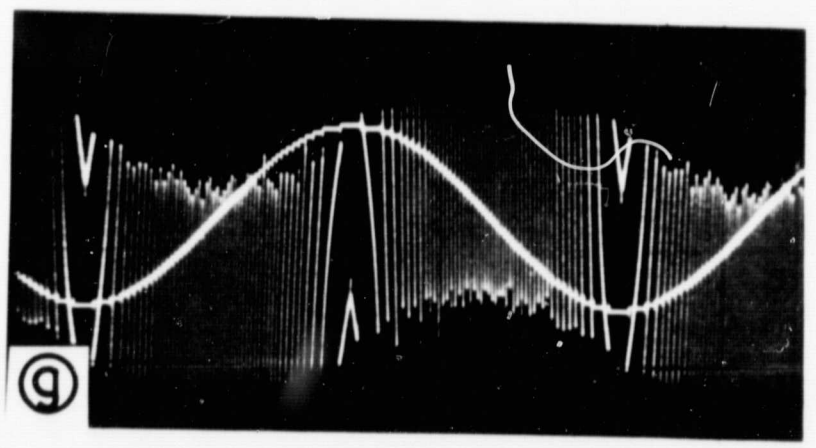

FIGURE 5

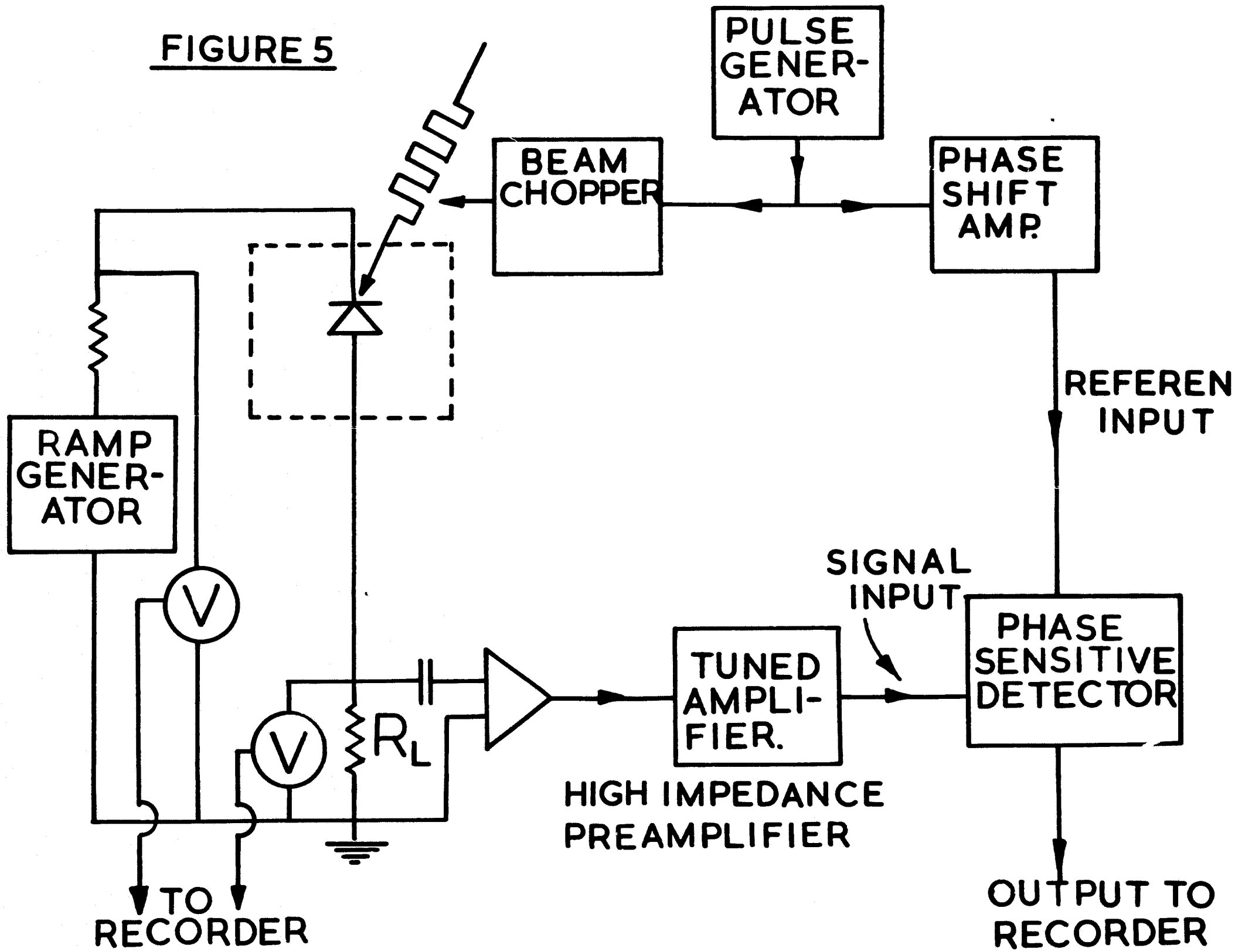
PULSE GENER-ATOR
BEAM CHOPPER
PHASE SHIFT AMP.
REFERENCE INPUT
RAMP GENER-ATOR
V
V
R_L
TUNED AMPLI-FIER.
SIGNAL INPUT
PHASE SENSITIVE DETECTOR
HIGH IMPEDANCE PREAMPLIFIER
TO RECORDER
OUTPUT TO RECORDER

FIGURE.6.

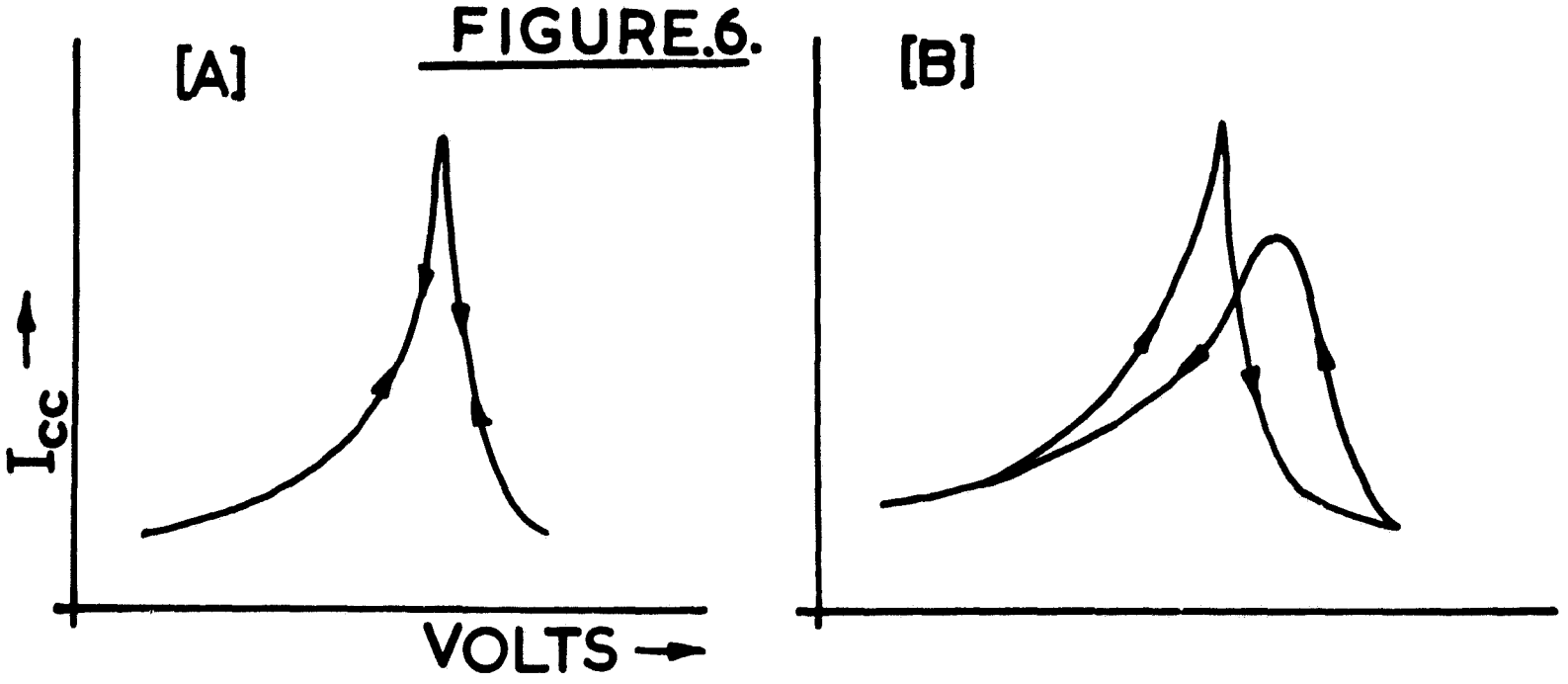

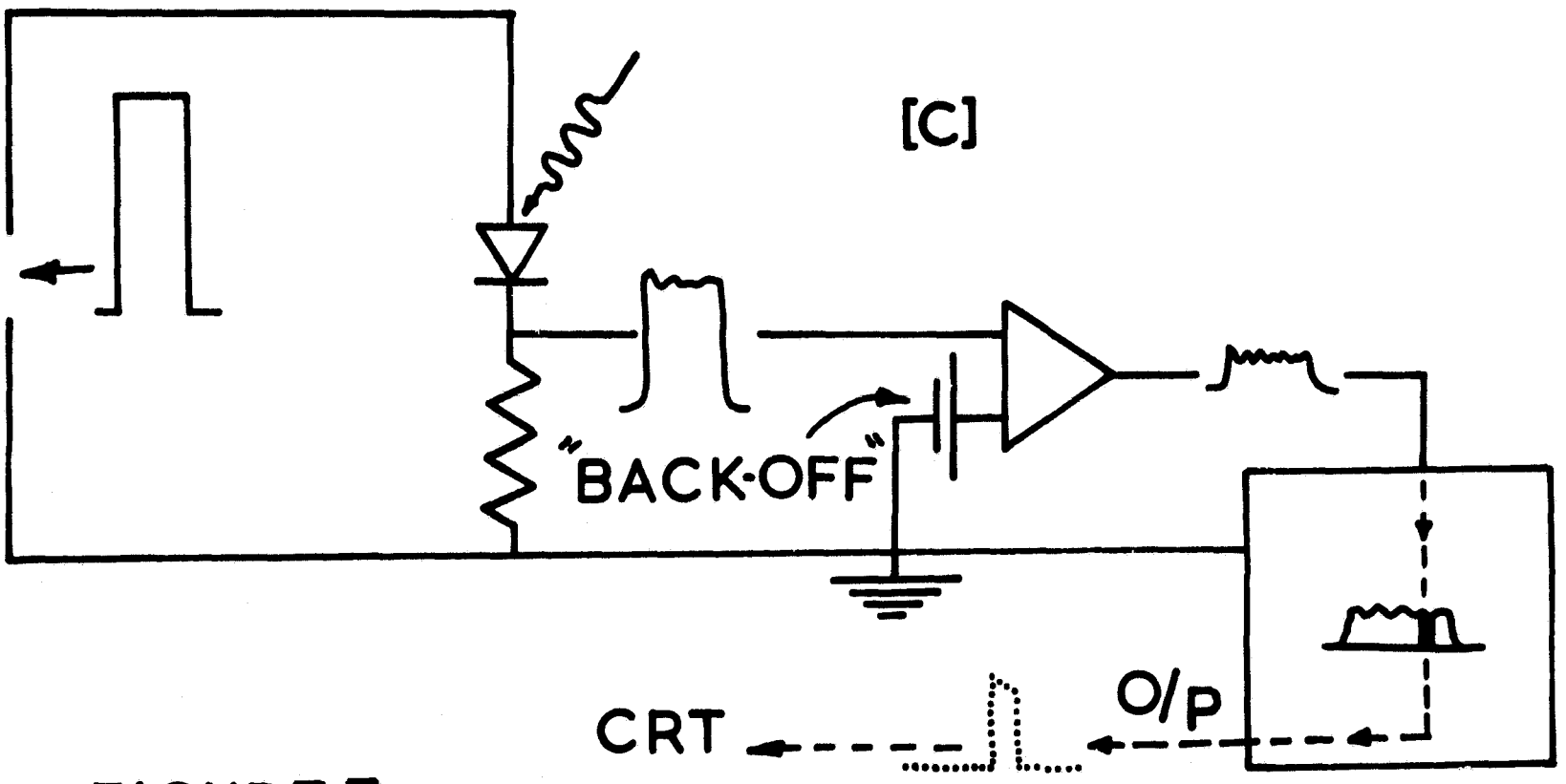

FIGURE.7.

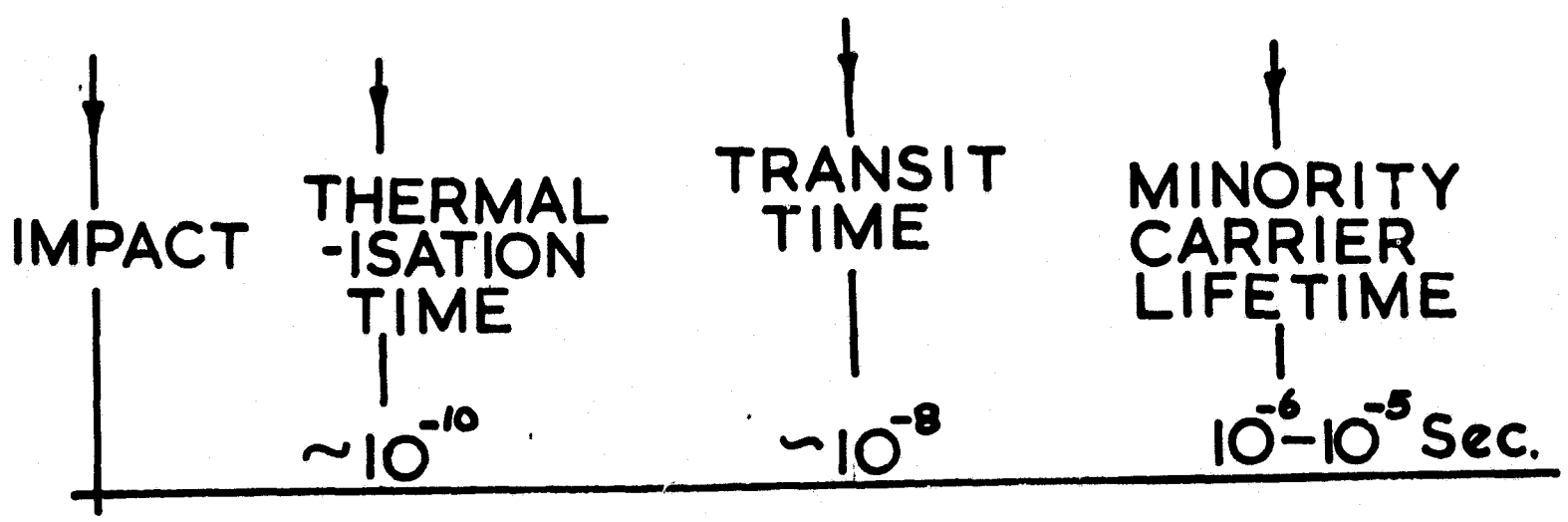

FIGURE.8.

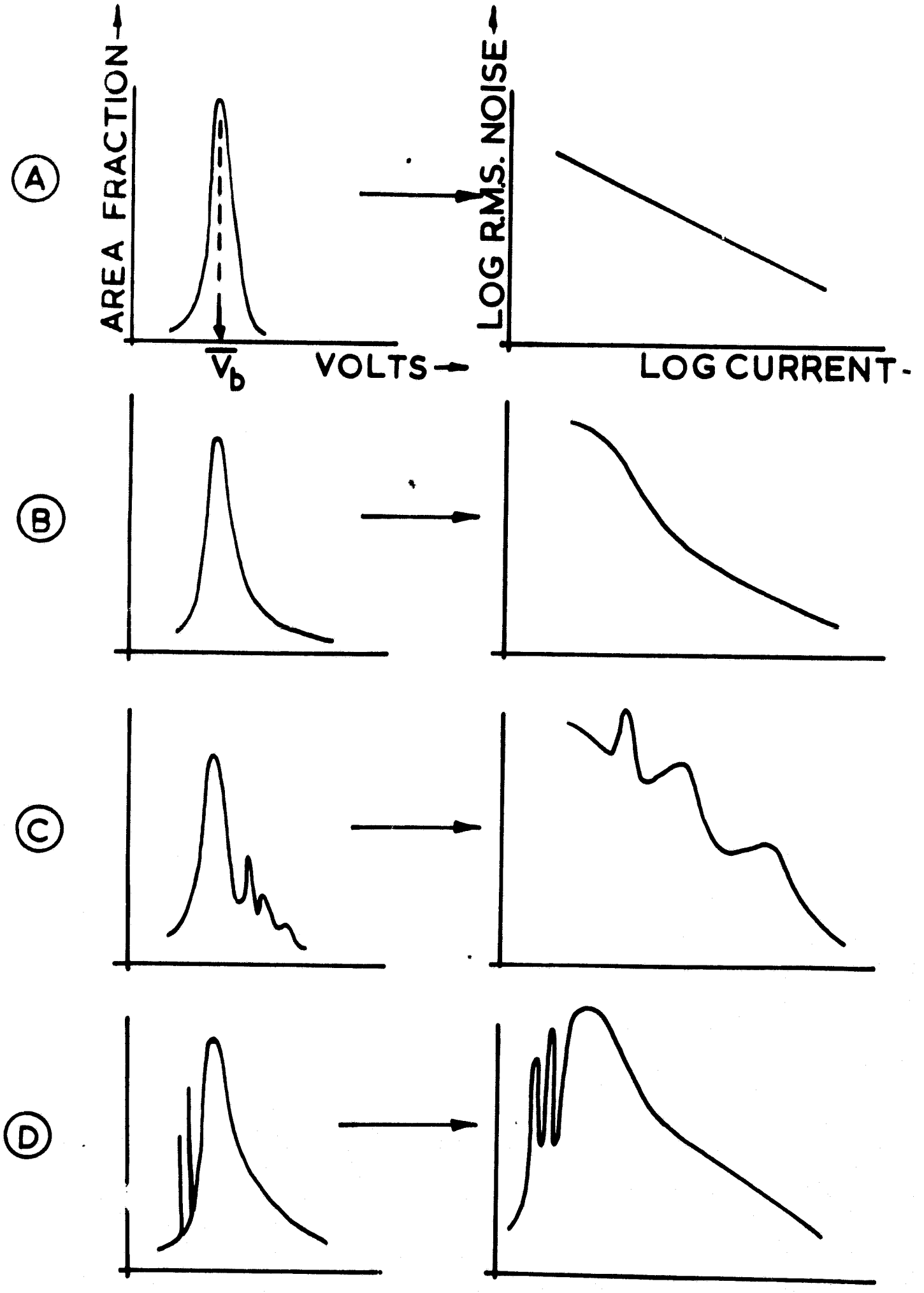

FIGURE.9.